

Short-term Backshore Processes under Wave and Wind Actions

K. Udo[†] and S. Yamawaki[‡]

[†]Disaster Control Research Center,
Tohoku University, Sendai
980-8573, Japan
udo@potential1.civil.tohoku.ac.jp

[‡]Chubu Regional Development Bureau, Ministry of Land, Infrastructure and Transport,
Nagoya
455-8545, Japan
yamawaki-s852a@pa.cbr.mlit.go.jp



ABSTRACT

UDO, K. and YAMAWAKI, S., 2007. Short-term backshore processes under wave and wind actions. *Journal of Coastal Research*, SI 50 (Proceedings of the 9th International Coastal Symposium), 237 – 241. Gold Coast, Australia, ISSN 0749.0208

Wave and wind impacts on short-term backshore processes were investigated through field observations of daily bed elevation, sand grain size, and wave, tide, and wind conditions at an open-ocean dissipative beach in Japan from September 2004 to March 2005. Indices of wave and wind impacts were defined by wave run-up level and wind-driven sand transport rate, respectively. The results show that waves have larger effects than winds on backshore sedimentation. Furthermore, both waves and winds cause sand coarsening in the backshore. Run-up waves are the external force with the greatest impact on backshore processes, followed by landward strong winds, and mild winds.

ADDITIONAL INDEX WORDS: *Rise of sea level, Littoral drift, Blown sand, Wave run-up, Sediment transport*

INTRODUCTION

Rising sea levels and increased storm intensities threaten beach and inland areas. The backshore plays an important role in protecting inland areas from coastal forces, serving as a site for beach recreation, and harboring rich ecosystems. Most studies of nearshore processes, however, have focused on foreshore and bar deformations caused by wave-driven sand transport.

The backshore is deformed not only by wind action, but also by wave action due to water level variations during extreme events such as typhoons, which cause large wave-induced erosion and sedimentation in the backshore. The elevation of mean high-water levels creates a transitional zone between the dune-related and wave-driven processes that affect the seasonal evolution of a dissipative beach (HAXEL and HOLMAN, 2004). Few studies of backshore processes, however, have considered both wave and wind actions.

Some studies have considered the effects of water level variations and wave-driven foreshore deformation on aeolian sand transport in the backshore. The aeolian sand transport rate and sediment supply to foredunes critically depend on the presence of dry sand sources as represented by well-drained intertidal bars (AAGAARD et al., 2004). Aeolian sand transport and upper beach/dune evolution is strongly controlled by the magnitude and frequency of high-water levels (RUZ and MEUR-FEREC, 2004).

UDO et al. (2006) conducted monthly field observations of backshore topography, sand grain size, and wave, tide, and wind conditions from September 2003 to February 2005 at an open-ocean beach in Japan. They demonstrated linkage of wave- and wind-driven sand transport in the backshore. The bed elevation change in the seaward area of the backshore was caused by both wave and wind actions. Spatial distributions of sand grain size

showed sand coarsening processes in the backshore, and both waves and winds cause the coarsening. They investigated wave and wind impacts on medium-term backshore processes; however, the detailed processes remain unclear. In this study, field observations of daily beach profile, sand grain size, and wave, tide, and wind conditions were conducted for the period September 2004 to March 2005 at the same beach as Udo et al. (2006), and more detailed wave and wind impacts were investigated in the short-term period.

STUDY AREA

The field observations were conducted at Hasaki Oceanographical Research Station (HORS), which faces the Pacific Ocean, in Japan (35°50'25" N – 140°45'42" E, Figure 1). Hasaki Beach is a dissipative beach with a foreshore slope of 0.02 to 0.04 (Fig. 2). The longshore distance $x = 130$ m is 130 m from a HORS research pier on the Choshi side. The predominant wind direction is landward from north to east-northeast. Waves and winds are relatively weak in summer except during typhoons, but strong in winter due to low pressure systems. The median sand grain size on the bed surface is approximately 0.2 mm. Beach grasses grow in the backshore and are especially thick around the sandbank at $y = -70$ m and the dune at $y = -130$ to -100 m.

METHODS

The field observations focused on beach profile, sand grain size on the bed surface, mean wave run-up level, and wave, tide, and wind conditions as shown in Table 1. All level data are based on the HORS datum level (DL = TP (Tokyo Peil) – 0.687 [m]). Short-term field data of bed elevation and sand grain size were

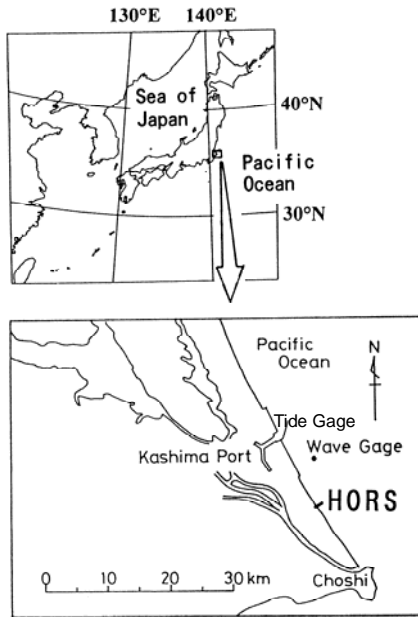


Figure 1. Location of study area (HORS) and wave and tide gages.

obtained at $y = -10, -50, -90,$ and -130 m (points A, B, C, and D shown in Figure 2, respectively) every day except on holidays from September 2004 to March 2005. The average wave run-up position in the observation period was $y = -10$ m in the cross-shore distance.

The bed elevation z (Data 1) was measured with a total station having an accuracy of ± 5 mm. The median grain size of sand, D_{50} (Data 2) was measured using a stack of successively finer sieves with meshes of 1.00ϕ (0.500 mm), 1.25ϕ (0.425 mm), 1.50ϕ (0.354 mm), 1.75ϕ (0.300 mm), 2.00ϕ (0.250 mm), 2.25ϕ (0.212 mm), 2.50ϕ (0.180 mm), 2.75ϕ (0.150 mm), 3.00ϕ (0.125 mm), 3.25ϕ (0.105 mm), and 3.75ϕ (0.075 mm), where the phi (ϕ) scale (KRUMBEIN, 1936) was used.

Indices of the wave and wind impacts were defined as the wave run-up level and wind-driven sand transport rate, respectively. Figure 3 shows a diagram of the wave run-up height (R_T), swash (R_S), wave setup (η), still-water level (SWL), and wave run-up level ($R_T + SWL$). The SWL was defined by the mean water level. The R_T was estimated using significant wave height, similar to the method of GUZA and THORNTON (1981, 1982), who reported that the wave run-up height could be estimated using the significant wave height at Torrey Pines Beach, California.

Table 1: Summary of field observation.

Data	Material	Instrument	Sampling period and point
1	z	Total station	Daily (September 2004 – March 2005), 4 points
2	D_{50}	Set of sieves	Daily (September 2004 – January 2005), 4 points
3	$R_T + SWL$	Visual observation	Irregularly (January 1997 – February 1998, January 2005)
4	$H_{1/3}$	Ultrasonic wave gauge	Twice hourly, $35^{\circ}53'55''$ N – $140^{\circ}45'14''$ E
5	SWL	Fuess-type tide gauge	Hourly, $35^{\circ}55'46''$ N – $140^{\circ}41'38''$ E
6	U_m and α_m	Propeller-type anemometer	Hourly, 10-m height above HORS datum level (= TP – 0.687)

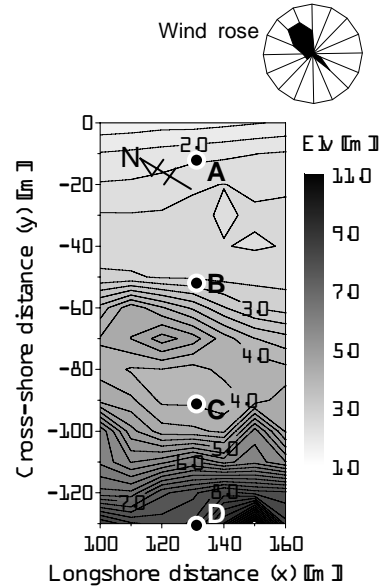


Figure 2. Topography of 17 Dec 2004 with a wind rose in the measurement period. Points A – D are measurement points.

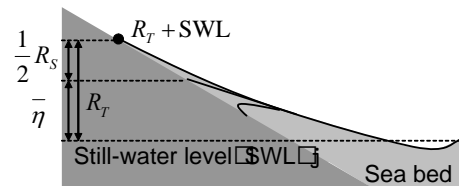


Figure 3. Diagram of mean wave run-up height (R_T), swash (R_S), wave setup (η) and wave run-up level ($R_T + SWL$).

Figure 4 shows the relationship between observed R_T and significant wave height $H_{1/3}$ (Data 4) for the period 1997 – 1998 at the study area. The observed R_T was calculated with the $R_T + SWL$ (Data 3) and SWL (Data 5). The value of $R_T + SWL$ was observed visually. The SWL and $H_{1/3}$ were measured hourly at Kashima Port with a Fuess-type tide gauge and twice hourly in 24-m-deep water with an ultrasonic wave gauge, respectively (Figure 1 and Table 1). As shown in Figure 4, R_T had a strong correlation with $H_{1/3}$ in deep water (correlation coefficient $r = 0.77$). The linear approximation is expressed as follows:

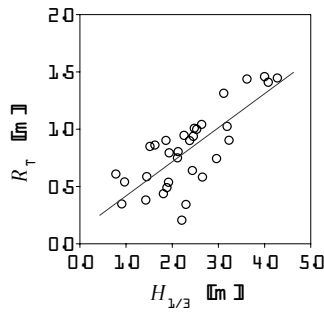


Figure 4. Relationship between the mean wave run-up height (R_T) and significant wave height in deep water ($H_{1/3}$).

$$R_T = 0.38H_{1/3} \quad (2)$$

Figure 5 shows time series of $H_{1/3}$, SWL at the Kashima Port and HORS, and the estimated and observed $R_T + SWL$ during an extreme event from 11 to 21 January 2005. The SWL at the Kashima Port was roughly the same as that at HORS in 6-m-deep water (Figure 5b). Equation (2) estimates the $R_T + SWL$ with good accuracy compared to the observed $R_T + SWL$ (Figure 5c).

The wind-driven sand transport rate q [$m^3/m/s$] was estimated using the 10-min mean wind speed and direction (Data 6) measured hourly with a propeller-type anemometer and using the following equations (Bagnold, 1941; Owen, 1964):

$$q = \zeta \frac{\rho}{\rho_s g} u_* (u_*^2 - u_{*t}^2) \quad (3)$$

$$\zeta = 0.25 + 1.66(\rho_s g d)^{1/2} / 3u_* \quad (4)$$

$$u_* = \kappa u_z / \log(z_a / z_0) \quad (5)$$

$$u_{*t} = A \sqrt{gd(\rho_s - \rho) / \rho} \quad (6)$$

where ζ is a constant, u_* is wind shear velocity, u_{*t} is threshold wind shear velocity, g is gravity ($= 9.81$ [m/s^2]), ρ is air density ($= 1.226$ [kg/m^3]), ρ_s is sand density ($= 2650$ [kg/m^3]), d is sand grain size ($= 0.2 \times 10^{-3}$ [m]), κ is the Karman coefficient ($= 0.41$), u_z is wind velocity at a height of z_a , z_a is the height of the anemometer based on the representative backshore elevation ($= 10 - 3 = 7$ [m]), z_0 is the aerodynamic roughness length ($= d/30$ [m]), and A is a coefficient ($= 0.1$). Equations (3) and (4) were used to calculate q when u_* (equation [5]) exceeded the threshold u_{*t} (equation [6]). The q was summed daily, and the daily cross-shore transport rate Q_y was obtained from the wind direction. Although sand transport is affected by the water content of the sand, visual observations showed that a large amount of dry sand is transported due to abrasion of the superficial humid sand layer when strong winds blow. Thus, the effect of water content was neglected in this study.

RESULTS

Figure 6 shows time series of daily ϕ of the median sand grain size D_{50} , the daily bed elevation at $y = -10, -50, -90,$ and -130 m (points A, B, C, and D shown in Figure 2, respectively), the twice-hourly wave run-up level $R_T + SWL$ and the bed elevation at $y = -10$ and -50 m, and the daily wind-driven sand transport rate Q_y in the cross-shore direction for the period September 2004 – March 2005. Observations of ϕ took place from September 2004 to January 2005. The bed elevation in Figure 6b is also based on that of 2 September 2004, and the elevation at $y = -10$ m is also based on values for 22 October 2004, 19 January 2005, and 14 February 2005 when notable wave-driven erosion occurred. The values of $R_T + SWL$ and Q_y were estimated using equations (2) – (6).

The variation in ϕ and bed elevation increased seaward as shown in Figures 6a and 6b. In particular, the ϕ varied daily and notably. Udo et al. (2006) showed that monthly spatial distribution change in sand grain size could be traced for one event, but not the other events, and this is because of the short-term variation. Standard deviations of the ϕ were 0.21 at $y = -10$ m, 0.18 at -50 m, 0.09 at -90 m, and 0.07 at -130 m, respectively.

The bed elevation tended to increase at $y = -50$ and -130 m except during the wave run-up period, whereas decrease at $y = -90$ m. These sedimentations and erosion were attributable to sand trapping by the sandbank and dune at $y = -70$ and -130 m, respectively. UDO et al. also pointed out the sand trapping. Waves

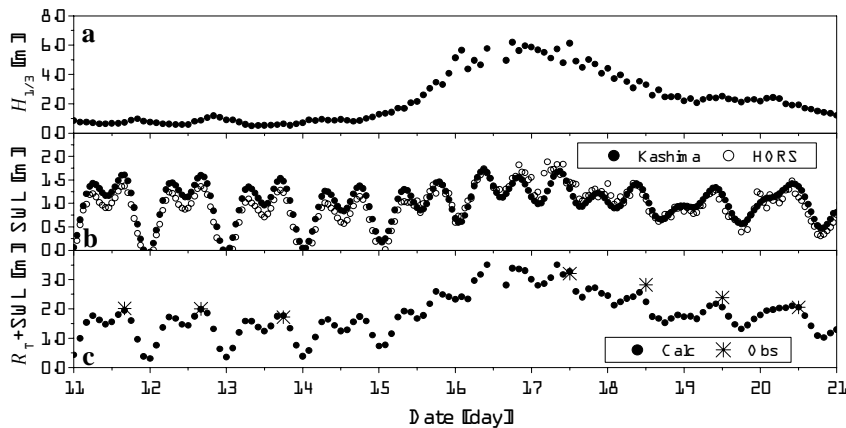


Figure 5. Time series of (a) significant wave height ($H_{1/3}$), (b) still water level (SWL) at Kashima Port and HORS, and (c) estimated and observed wave run-up level ($R_T + SWL$) during 11 – 21 January 2005.

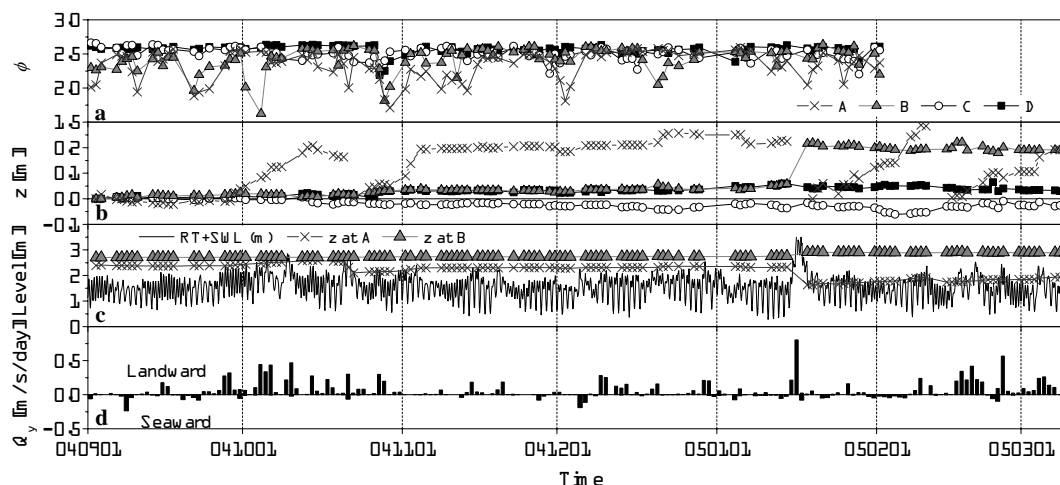


Figure 6. Time series of (a) daily ϕ of D_{50} , (b) daily bed elevation at $y = -10, -50, -90,$ and -130 m (points A, B, C, and D shown in Fig. 2, respectively) based on that on 2 September 2004, (c) twice-hourly wave run-up level $R_T + SWL$ and the bed elevation at $y = -10$ and -50 m, and (d) daily wind-driven sand transport rate Q_y , in the period September 2004 – March 2005. The elevation at $y = -10$ m is also based on that on 22 October 2004, 19 January 2005, and 14 February 2005 when notable wave-driven erosion occurred.

acted on the beds at $y = -10$ and -50 m and caused notable bed elevation changes as shown in Figures 6b and 6c. The bed elevation tended to increase just after the bed erosion in the periods 20 October – 4 November 2004, 14 January – 9 February 2005, and 14 – 25 February 2005. The bed elevation change under wave action was much larger than those under wind action.

Table 2 shows conditions of bed elevation, wave, and wind when the sand was coarsened by more than 25% in 5 days. The landward and seaward ΣQ_y from one measurement date to the next were obtained by the sum of Q_y over the period. Considering that wave action is a much more effective transporter of sand than wind, external forces of the sand coarsening can be classified into three types in order of their impacts on backshore processes: (i) run-up waves, (ii) strong landward winds, and (iii) mild winds.

Strong winds were defined as $\Sigma Q_y > 0.2 \text{ m}^3/\text{m}$. The coarse sand became finer within 2 weeks independent of the wind condition.

DISCUSSION

Figure 7 shows the relationship between bed elevation change due to wave run-up and specific energy (total head) at $y = -10$ and -50 m. The specific energy was defined as the wave run-up level based on the bed elevation. The bed elevation tended to increase when the specific energy was small, but decrease with an increase in the specific energy. The sedimentation occurred at the higher level of eroded area simultaneously with the notable erosion as reported by KATOH and YANAGISHIMA (1992). These results suggest that sand eroded by strong waves is transported landward and deposits around the seaward edge of the run-up wave.

Table 2: Sand coarsening by more than 25% in 5 days.

Class	Date	y [m]	ϕ	z [m]	$(R_T + SWL)_{\max}$ [m], $\Sigma Q_y(L, S)$ [m^3/m]
(iii)	8 – 10 Sep 04	-10	2.46→1.94	2.381→2.379	1.62, (0.001, 0.033)
(iii)	17 – 21 Sep 04	-50	2.45→1.96	2.711→2.714	1.93, (0.000, 0.082)
(iii)		-10	2.57→1.89	2.368→2.384	
(ii)	30 Sep – 4 Oct 04	-50	2.51→1.62	2.725→2.719	2.51, (0.558, 0.008)
(i)	19 – 21 Oct 04	-10	2.50→2.00	2.555→2.319	2.66, (0.293, 0.060)
(ii)		-130	2.63→2.19	8.036→8.055	
(ii)	26 – 28 Oct 04	-50	2.55→1.81	2.724→2.731	2.29, (0.442, 0.000)
(i)		-10	2.30→1.83	2.147→2.157	
(iii)	10 – 11 Nov 04	-50	2.55→2.15	2.734→2.735	1.84, (0.000, 0.000)
(iii)	27 Nov – 2 Dec 04	-10	2.46→1.81	2.305→2.285	1.99, (0.052, 0.015)
(ii)	16 – 20 Dec 04	-50	2.58→2.05	2.735→2.756	2.25, (0.199 , 0.010)
(i)	14 – 18 Jan 05	-10	2.40→2.04	2.325→1.635	3.50, (0.974, 0.073)
(i)	21 – 25 Jan 05	-10	2.52→2.06	1.695→1.691	2.03, (0.019, 0.035)

External forces on sand coarsening are classified into (i) run-up waves, (ii) strong landward winds, and (iii) mild winds. The z is the bed elevation, $(R_T + SWL)_{\max}$ is the daily maximum wave run-up level, and $\Sigma Q_y(L, S)$ represents the landward and seaward wind-driven sand transport rates. The values in bold show changes of z larger than 0.2 m, wave run-up landward of $y = -10$ m, and ΣQ_y larger than $0.2 \text{ m}^3/\text{m}$.

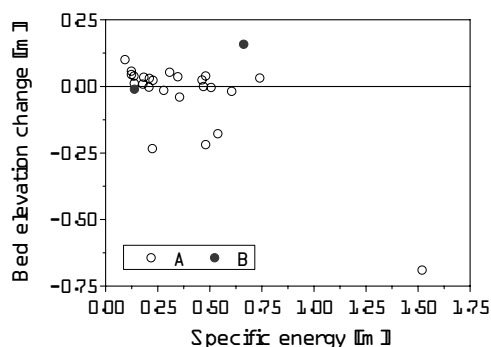


Figure 7. Relationship between bed elevation change under wave action and specific energy (total head) at $y = -10$ and -50 m (points A and B shown in Fig. 2, respectively).

Although the bed elevation change was most likely influenced by wave conditions, the wave condition could not be specified for the bed erosion and sedimentation. Figure 8 shows the bed elevation, wave run-up level (R_T+SWL), significant wave height ($H_{1/3}$), and infragravity wave height ($SLH_{1/3}$) at $y = -10$ m during the period 27 September – 6 November 2004. The $SLH_{1/3}$ was defined by waves with power spectral densities in frequencies lower than 0.033 Hz. The maximum $H_{1/3}$ and $SLH_{1/3}$ for the period T_1 were not less than those for the period T_2 ; however, the bed elevation increased for the period T_1 and decreased for the period T_2 . More detailed wave analyses, e.g. duration of high infragravity waves, are needed to determine the erosion and sedimentation mechanisms.

Considering that the external forces on sand coarsening can be classified into (i) run-up waves, (ii) strong landward winds, and (iii) mild winds and that the coarse sand became finer within 2 weeks independent of the wind condition, the mechanisms of sand coarsening in the backshore can be explained as follows. At first, coarse sand is transported with fine sand to the foreshore or the seaward part of the backshore by wave run-up. Under strong landward winds, both coarse and fine sands are transported landward and sand coarsening occurs in the backshore. On the other hand, under mild winds, only the fine sand is transported and coarsening occurs in the area of the wave run-up. After coarsening, the sand becomes finer due to diffusion of the coarse sand, mixture of coarse and fine sands during transport, or sedimentation of fine sand on the coarse sand. These processes suggest that both wave and wind actions contribute to sand coarsening.

CONCLUSION

This study examined small-scale backshore processes based on field observations of bed elevation, sand grain size, wave run-up, and wind-driven sand transport rate.

The bed elevation change in the seaward area of the backshore was caused by both wave and wind actions, and the wave impact on the backshore process was larger than the wind impact.

The variation in sand grain size increased seaward, indicating that coarse sand was moved by strong waves to the foreshore and by winds to the backshore. Both waves and winds cause sand coarsening. The coarse sand became finer within 2 weeks independent of the wind condition.

External forces acting on backshore processes are classified as run-up waves, landward strong winds, and mild winds.

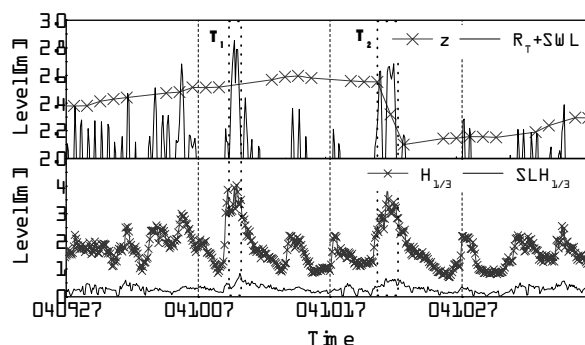


Figure 8. Wave condition for bed erosion and sedimentation at $y = -10$ m during the period 27 September – 6 November 2004. The $SLH_{1/3}$ is infragravity wave height.

ACKNOWLEDGEMENTS

The offshore wave and tide data were provided by Kashima Port Construction Office of Ministry of Land, Infrastructure and Transport. The wave run-up and wind data at HORS were provided by Littoral Drift Division of Port and Airport Research Institute. This research was funded by the Ministry of Education, Culture, Sports, Science and Technology, Grant-in-Aid for Young Scientists (B) #16760417. The authors would like to thank two reviewers for their thorough reviews.

LITERATURE CITED

- AAGAARD, T., DAVIDSON-ARNOTT, R., GREENWOOD, B. and NIELSEN, J., 2004. Sediment supply from shoreface to dunes: linking sediment transport measurements and long-term morphological evolution. *Geomorphology*, 60(1-2), 205–224.
- BAGNOLD, R.A., 1941. The physics of blown sand and desert dunes. Methuen, London, 265p.
- GUZA, R.T. and THORNTON, E.B., 1981. Wave set-up on a natural beach. *Journal of Geophysical Research*, 86(C5), 4133–4137.
- GUZA, R.T. and THORNTON, E.B., 1982. Swash oscillations on a natural beach. *Journal of Geophysical Research*, 87(C1), 483–491.
- HAXEL, J.H. and HOLMAN, R.A., 2004. The sediment response of a dissipative beach to variations in wave climate. *Marine Geology*, 206(1-4), 73–99.
- KATOH, K. and YANAGISHIMA, S., 1992. Berm formation and berm erosion. *Proceedings of the 23th Conference of Coastal Engineering* (Venice, Italy, ASCE), pp. 2136–2149.
- KRUMBEIN, W.C., 1936. Application of logarithmic moments to size frequency distribution of sediments. *Journal of Sedimentary Petrology*, 6(1), 35–47.
- OWEN, P.R., 1964. Saltation of uniform grains in air. *Journal of Fluid Mechanics*, 20(2), 225–242.
- RUZ, M-H. and MEUR-FEREC, C., 2004. Influence of high water levels on aeolian sand transport: upper beach/dune evolution on macrotidal coast, Wissant Bay, northern France. *Geomorphology*, 60(1-2), 73–87.
- UDO, K., YAMAWAKI, S. and ITO, Y., 2006. Temporal changes of backshore topography and sand grain size under wind and wave actions. *Proceedings of the 30th Conference of Coastal Engineering* (San Diego, USA, ASCE). (in press)